# Open Archive TOULOUSE Archive Ouverte (OATAO)

OATAO is an open access repository that collects the work of Toulouse researchers and makes it freely available over the web where possible.

# Large specific absorption rates in the magnetic hyperthermia properties of metallic iron nanocubes

B. Mehdaoui [a,b], A. Meffre [a,b], L.-M. Lacroix [a,b], J. Carrey [a,b,*], S. Lachaize [a,b], M. Gougeon [c], M. Respaud [a,b], B. Chaudret [d]

[a] Université de Toulouse, INSA, UPS, LPCNO (Laboratoire de Physique et Chimie des Nano-Objets), 135 avenue de Rangueil, F-31077 Toulouse, France
[b] CNRS, UMR 5215, LPCNO, F-31077 Toulouse, France
[c] Institut CARNOT-CIRIMAT-UMR 5085, Bâtiment 2R1, 118 route de Narbonne, F-31062 Toulouse, France
[d] Laboratoire de Chimie de Coordination-CNRS, 205 rte de Narbonne, 31077 Toulouse cedex 4, France

## ABSTRACT

We report on the magnetic hyperthermia properties of chemically synthesized ferromagnetic 11 and 16 nm Fe(0) nanoparticles of cubic shape displaying the saturation magnetization of bulk iron. The specific absorption rate measured on 16 nm nanocubes is $1690 \pm 160$ W/g at 300 kHz and 66 mT. This corresponds to specific losses-per-cycle of 5.6 mJ/g, largely exceeding the ones reported in other systems. A way to quantify the degree of optimization of any system with respect to hyperthermia applications is proposed. Applied here, this method shows that our nanoparticles are not fully optimized, probably due to the strong influence of magnetic interactions on their magnetic response. Once protected from oxidation and further optimized, such nano-objects could constitute efficient magnetic cores for biomedical applications requiring very large heating power.

## 1. Introduction

Magnetic hyperthermia is a way to improve the efficiency of chemotherapy or radiotherapy by raising the temperature of a tumour to 41–45 °C during a few hours using magnetic nano-particles (MNPs). In the clinical treatment set at the Charité Hospital, Berlin, MNPs are first localised inside the tumour and then excited by an alternating magnetic field of moderate amplitude $\mu_0 H_{app}$ (12–25 mT) at a frequency $f_{exc}$ of 100 kHz [1]. The power released by the NPs is assessed by their specific absorption rate (SAR) or their specific losses-per-cycle (SLPC) noted $A$, linked by the equation $SAR = A f_{exc}$. Increase in SARs above 1 kW/g could be beneficial for several aspects of the hyperthermia applications but it implies a real challenge [2]. Indeed, due to physiological issues, human body cannot be exposed to alternating magnetic field of large $H_{app}f_{exc}$ product [2]. Therefore, the optimization of the treatment must rely on the MNPs only. The most favourable case, leading to $SAR_{max} = 4\mu_0 H_{app}\sigma_S f_{exc}$ occurs when (i) the magnetization loop, characterized by a coercive field $H_C$ and a saturation magnetization per unit mass $\sigma_S$, is a perfect square and (ii) $H_C \approx H_{app}$. Unfortunately, due to the random

orientations of easy axis, to magnetic interactions and to thermal activation, hysteresis loops of MNPs assemblies are far from being square. Thus, more generally, one can write

$$SAR = 4\alpha\mu_0 H_{app}\sigma_S f_{exc} \qquad (1)$$

where $\alpha$ is a dimensionless parameter, which characterizes the relative area of the hysteresis loops with respect to the ideal square. As a consequence of Eq. (1) and of the limitation of the $H_{app}f_{exc}$ product, the maximisation of the SAR requires MNPs displaying a high $\sigma_S$ and hysteresis loops as square as possible (large $\alpha$).

High magnetization materials are essentially metallic Ni, Fe, Co and their alloys. Among them, iron is the most promising one since it displays a very large $\sigma_S$ and is *a priori* the most biocompatible. However, iron oxides have been so far the most widely studied materials for magnetic hyperthermia, due to their full biocompatibility and the relative simplicity of their synthesis and handling. Optimized chemically synthesized $Fe_3O_4$ NPs have shown SLPC up to 1.5 mJ/g at 400 kHz [3]. Among high magnetization materials, higher SLPC values up to 3.2 mJ/g at 400 kHz have been reported for Co MNPs [4]. The scarce results published so far on Fe MNPs are disappointing as a consequence of the lack of control of the surface oxidation and/or of a non-optimal nanoparticle size [5–7]. The best results published so far were performed on $Fe/Fe_xO_y$ core–shell MNPs, which displayed low $\sigma_S$ and SLPC comparable to those measured on iron oxides [5].

* Corresponding author at: Université de Toulouse, INSA, UPS, LPCNO (Laboratoire de Physique et Chimie des Nano-Objets), 135 avenue de Rangueil, F-31077 Toulouse, France.
E-mail address: julian.carrey@insa-toulouse.fr (J. Carrey).

Our group has developed an organometallic approach allowing the controlled synthesis of pure metallic iron NPs displaying the bulk magnetization [8–10]. We report in this article on the magnetic and hyperthermia measurements of ferromagnetic 11 and 16 nm nanocubes exhibiting very large SLPC. Their efficiency for the required application and the influence of magnetic interactions on this efficiency is discussed.

## 2. Synthesis and characterzations

The two samples of Fe nanocubes were synthesized by a two steps organometallic route, which has been previously reported [8]. A complete description of the size and shape control on iron NPs synthesized by this route will be published elsewhere. First, we prepared small Fe particles (∼2 nm) through the
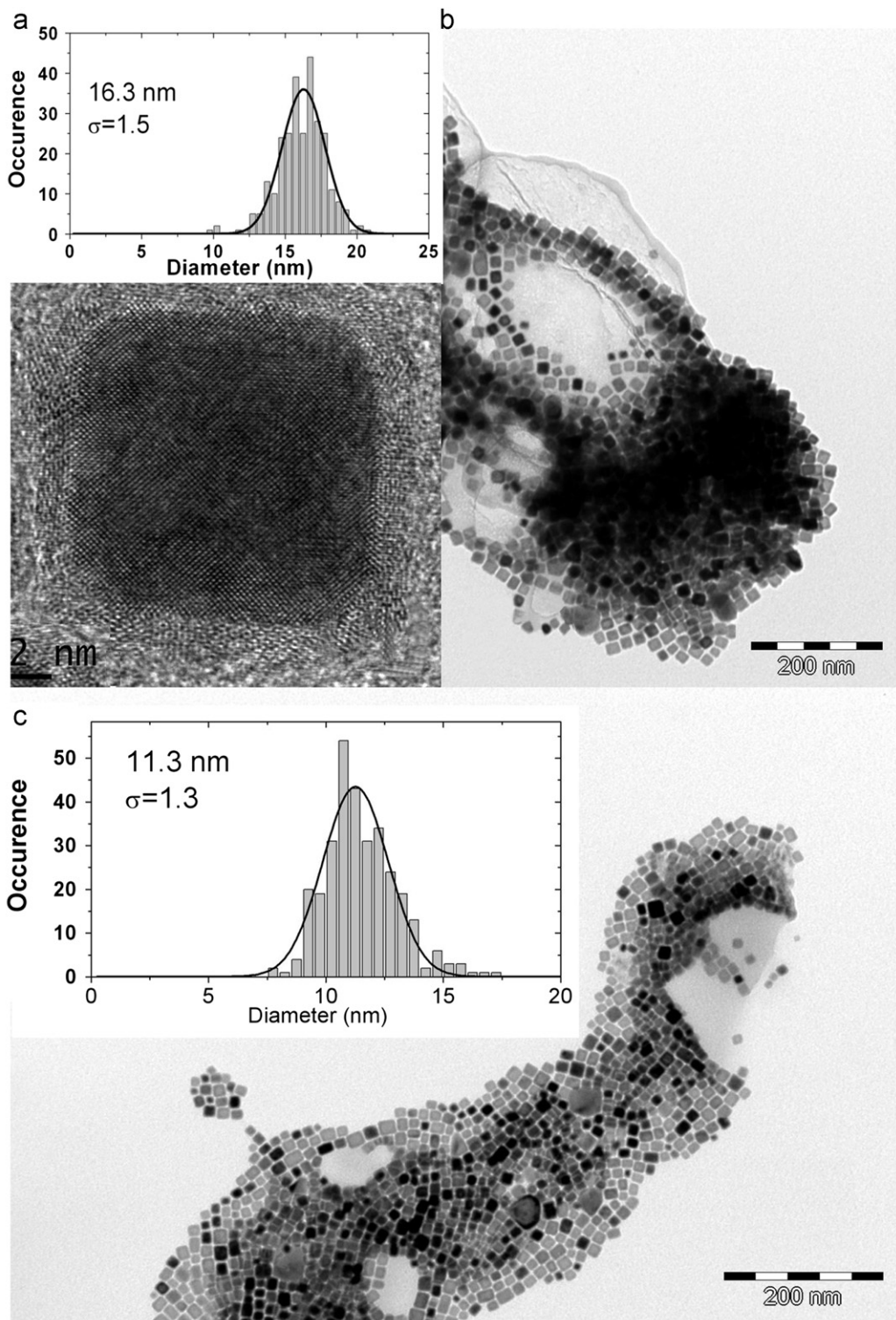


**Fig. 1.** TEM micrographs of the iron nanocubes measured in hyperthermia. (a) High-resolution TEM micrograph on an isolated nanocube in sample 1. (b) Sample 1: nanocubes with a mean diameter of 16.3 nm. (c) Sample 2: nanocubes with a mean diameter of 11 nm. Insets: nanocube size distribution extracted from the analysis of several TEM micrographs.
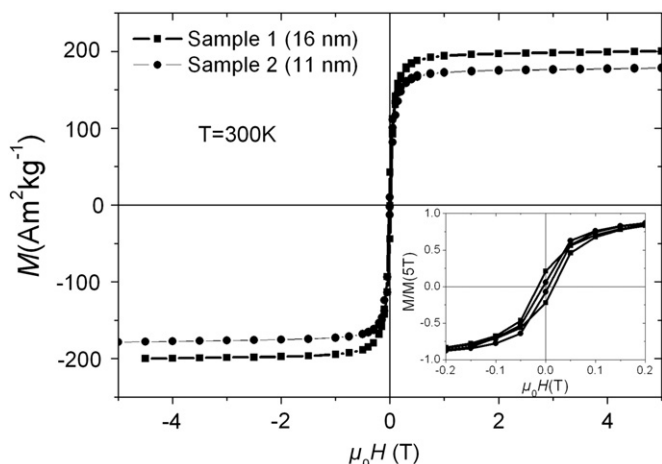
**Fig. 2.** SQUID measurement at 300 K on sample 1 (16 nm) and sample 2 (11 nm). The inset shows an enlarged view of the magnetization normalized by its value at 5 T.

decomposition of the iron dimer $\{Fe[N(SiMe_3)_2]_2\}_2$, (376 mg, 0.5 mmol) in mesitylene (20 mL) at 150 °C under 3 bars of $H_2$ in a Fisher–Porter bottle (170 mL) [11]. In a second step, a mixture of hexadecylammonium chloride (HDA·HCl) and hexadecylamine (HDA) was added to the colloidal solution. For sample 1, the ratio ammonium/amine was 1:2 (277 mg, 1 mmol HDA·HCl; 483 mg, 2 mmol HDA). For sample 2, this ratio was 1.1:2 (304.7 mg, 1.1 mmol HDA·HCl; 483 mg, 2 mmol HDA). The solution was stirred for 20 min at 90 °C then pressurised under 3 bars of $H_2$ and heated at 150 °C. After 48 h, a black precipitate was formed at the bottom of the Fisher–Porter bottle. The solvent was filtered off and the precipitate was washed three times with 15 mL of toluene to remove the surfactants in excess and other remaining molecular species. The final iron content was 71% and 88% for samples 1 and 2, respectively, as determined by chemical analysis.

Samples for transmission electron microscopy (TEM) were prepared by the deposition of a drop of solution onto a carbon-coated copper grid. High-resolution TEM revealed that the nanocubes were single-crystalline and exhibited a bcc crystal structure, with facets of (1 0 0) planes (see Fig. 1(a)). As revealed by TEM micrographs, most of the nanocubes were embedded in organic mesophases, which prevent them to form a true colloidal solution (see Figs. 1(b) and 1(c)). Similar nanocube-filled mesophases have already been characterized for a similar system in which carboxylic acid was used instead of ammonium chloride [9]. Size distributions measured from several TEM micrographs showed that samples 1 and 2 were composed of iron nanocubes of mean side lengths $16.3 \pm 1.5$ nm (sample 1) and $11.3 \pm 1.3$ nm (sample 2), respectively, (see insets of Fig. 1(b) and (c)).

Samples for magnetic measurements were prepared and sealed under an argon atmosphere in order to preserve the metallic character of Fe. SQUID measurements on powders of samples 1 and 2 are shown in Fig. 2. Their saturation magnetizations per unit mass $\sigma_S$ were $200 \pm 10$ and $178 \pm 9$ Am$^2$/kg at 300 K, respectively, just below the bulk value. Their coercive fields $H_C$ at 300 K are 16 and 5 mT, respectively.

## 3. Hyperthermia measurements

Hyperthermia experiments were performed on an induction oven working at a frequency of 300 kHz and a maximum magnetic field of 66 mT. For hyperthermia measurements, an

ampoule containing the colloidal solution was sealed under vacuum to prevent any oxidation of the NPs. A typical ampoule contains 9 mg of powder and 550 mg of mesitylene. The ampoule was then placed into a calorimeter with 1.5 mL of deionised water, the temperature of which was measured. The measurement time was adjusted between 20 and 200 s depending on the experiment, so that the temperature rise never exceeds 20 °C. After the magnetic field stops, the water is shaken during roughly 20 s to ensure the ampoule thermalization and the homogeneity of the water temperature, which is checked by putting two probes at the top and the bottom of the calorimeter. The temperature rise is measured after this process. For measurements longer than 20 s, the raw SAR values were corrected from the calorimeter losses, which were previously calibrated. The SAR values at 66 mT and their error bars were obtained by averaging three measurements of 20 s on three different ampoules arising from the same MNP synthesis (9 values). The complete magnetic-field dependence of the SAR was measured on a single ampoule for each synthesis and its SAR value renormalized accordingly.

During hyperthermia experiments, the spatial organisation of the MNPs in the ampoule was completely redistributed by the application of the magnetic field. Indeed, while the MNPs aggregates fall down by gravity at the bottom of the ampoule in the absence of any applied magnetic field, the MNPs formed small spikes along the field direction when a small magnetic field was applied. Moreover, for larger magnetic fields, the MNPs self-organized into regularly spaced levitating needles, which disintegrated as soon as the magnetic field was stopped. This phenomenon is shown in Fig. 3(a) for sample 2. The magnetic field for which these needles formed ranged between 20 and 30 mT; it was higher for sample 1 than for sample 2. The formation of columns in a magnetic field is a classical behaviour of ferrofluids and is due to magnetic interactions between the MNPs [12].

Fig. 3(b) displays the SAR values at 300 kHz as a function of the applied magnetic field for the two samples. In both cases, SAR increases strongly in the range 10–30 mT and then follows a roughly linear increase at higher magnetic field without complete saturation. For sample 1, the increase is sharper and occurs at a higher magnetic field than for sample 2. Such an abrupt increase followed by a plateau is a typical feature of ferromagnetic samples and was previously reported on ferromagnetic FeCo MNPs [13]. The sharp rise of the SAR occurs when $\mu_0 H_{app}$ reaches the coercive field of the MNPs. SARs up to $1690 \pm 160$ and $1320 \pm 140$ W/g are measured at 66 mT for samples 1 and 2, respectively. For sample 1, this value corresponds to SLPC of $5.6 \pm 0.5$ mJ/g, which exceeds
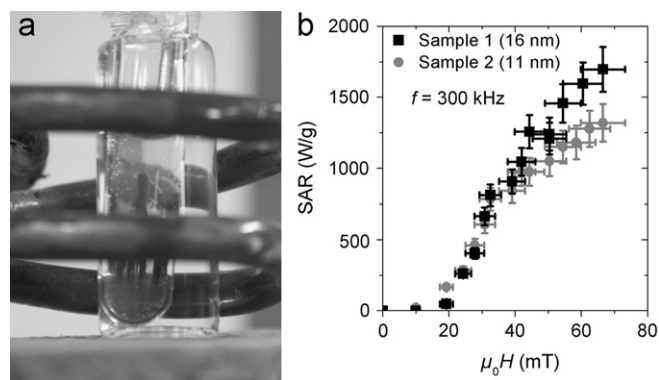


**Fig. 3.** (a) An hyperthermia experiment on sample 2 at a magnetic field of 66 mT and 300 kHz. The needles formed by the nanoparticles under the influence of the magnetic field are visible. (b) Magnetic field dependence of SAR at 300 kHz for the two samples.

by a factor 3 the values reported on optimized chemically synthesized iron oxide NPs [3].

## 4. Discussion on efficiency

The efficiency of our system is however limited for two reasons. First, the calculation of $\alpha$ at $\mu_0 H_{app} = 66$ mT using Eq. (1) with the experimental SAR value, and the experimental $\sigma_S$ value at 300 K leads to $\alpha = 0.11$ and $\alpha = 0.09$ for samples 1 and 2, respectively. Above $\mu_0 H_{app} = 32$ mT, $\alpha$ values are approximately constant with the magnetic field but decreases below. These values are rather low since a value up to $\alpha = 0.3$ can be deduced from the measurements on randomly oriented optimized iron oxide NPs [3]. In our case, this low $\alpha$ value is compensated by a larger $\sigma_S$. We argue that the presence of magnetic interactions is the main reason for these low $\alpha$ values. Indeed, in the case of the Stoner–Wohlfarth (SW) model, valid for randomly oriented magnetically independent nanoparticles, $\alpha_{SW} = 0.25$ [14]. When the nanoparticles interact magnetically, it is well admitted that both $H_C$ and $M_R$ decrease [15], thus reducing $\alpha$ below $\alpha_{SW}$. We are clearly in the presence of a system dominated by strong interactions since (i) the nanoparticles form dense needles when the magnetic field is on, (ii) the $M_R/M_S$ ratio ($M_R$ is the remnant magnetization and $M_S$ the saturation magnetization) in SQUID measurements is 0.2 and 0.06 for samples 1 and 2, respectively, whereas 0.5 is expected in the absence of interactions, (iii) the saturation field is well above $2H_C$. The second limitation of our system is that we measured huge SLPCs at a magnetic field of 66 mT while, so far, only magnetic fields close to 20 mT were applied during medical hyperthermia treatments [16]. A fine tuning of their size and/or of their dispersion must be considered to decrease their coercive field so that high SLPC values could be obtained at reduced magnetic field.

## 5. Conclusion

Our measurements of very large SARs on metallic iron NPs above 1 kW/g confirm the potential of high magnetization MNPs for future hyperthermia applications when large SAR would be required. However, progress in the control of their coercive field and of their magnetic interactions should be done. Furthermore, these nano-objects are not ready yet for biomedical applications since they should be protected from oxidation and their toxicity must be tested. To protect the metallic core from oxidation, a silica layer can be used, as recently patented by our group [17]. These non-trivial adjustments and post-treatments will constitute the future developments of this work.

## References

[1] P. Wust, U. Gneveckow, M. Johannsen, D. Böhmer, T. Henkel, F. Kahmann, J. Sehouli, R. Felix, J. Ricke, A. Jordan, Int. J. Hyperthermia 22 (2006) 673.
[2] R. Hergt, S. Dutz, J. Magn. Magn. Mater. 311 (2007) 187.
[3] R. Hergt, R. Hiergeist, I. Hilger, W.A. Kaiser, Y. Lapatnikov, S. Margel, U. Richter, J. Magn. Magn. Mater. 270 (2004) 345.
[4] M. Zeisberger, S. Dutz, R. Müller, R. Hergt, N. Matoussevitch, H. Bönneman, J. Magn. Magn. Mater. 311 (2005) 224.
[5] I. Baker, Q. Zeng, W. Li, C.R. Sullivan, J. Appl. Phys. 99 (2006) 08H106.
[6] Y. Krupskaya, C. Mahn, A. Parameswaran, A. Taylor, K. Krämer, S. Hampel, A. Leonhardt, M. Ritschel, B. Büchner, R. Klingeler, J. Magn. Magn. Mater. 321 (2009) 4067.
[7] B. Mehdaoui, A. Meffre, L.-M. Lacroix, J. Carrey, S. Lachaize, M. Respaud, M. Gougeon, B. Chaudret, J. Appl. Phys. 107 (2010) 09A324.
[8] F. Dumestre, B. Chaudret, C. Amiens, P. Renaud, P. Fejes, Science 303 (2004) 821.
[9] L.-M. Lacroix, S. Lachaize, A. Falqui, M. Respaud, B. Chaudret, J. Am. Chem. Soc. 131 (2009) 549.
[10] E. Snoeck, C. Gatel, L.M. Lacroix, T. Blon, S. Lachaize, J. Carrey, M. Respaud, B. Chaudret, Nano Lett. 8 (2008) 4293.
[11] L.-M. Lacroix, S. Lachaize, A. Falqui, T. Blon, J. Carrey, M. Respaud, F. Dumestre, C. Amiens, O. Margeat, B. Chaudret, P. Lecante, E. Snoeck, J. Appl. Phys. 103 (2008) 07D521.
[12] M. Klokkenburg, B.H. Erné, J.D. Meeldijk, A. Wiedenmann, A.V. Petukhov, R.P.A Dullens, A.P. Philipse, Phys. Rev. Lett. 97 (2006) 185702.
[13] L.-M. Lacroix, R. Bel Malaki, J. Carrey, S. Lachaize, M. Respaud, G.F. Goya, B. Chaudret, J. Appl. Phys. 105 (2009) 023911.
[14] R. Hergt, W. Andrä, C.G. d'Ambly, I. Hilger, W.A. Kaiser, U. Richter, H.-G. Schmidt, IEEE Trans. Magn. 34 (1998) 3745.
[15] D. Kechrakos, K.N. Trohidou, Phys. Rev. B 58 (1998) 12169.
[16] A. Jordan, R. Scholz, K. Maier-Hauff, M. Johannsen, P. Wust, J. Nadobny, H. Schirra, H. Schmidt, S. Deger, S. Loening, W. Lanksch, R. Felix, J. Magn. Magn. Mater. 225 (2001) 118.
[17] F. Delpech, C. Nayral, N. El Hawi, WO/2009/071794.